DOI: 10.48011/sbse.v1i1.2491

Adaptive Perturb and Observe with Simulated Annealing for the Maximum Power Point Tracking of Photovoltaic Modules in Multiple Shading Scenarios

Rafael M. R. Praxedes, * **Luciano S. Barros,** *
Clauirton A. Siebra, * **Camila M. V. Barros** *

* *Federal University of Paraíba, João Pessoa-PB, Brazil (e-mail: rafaelpraxedes@eng.ci.ufpb.br, lsalesbarros@gmail.com, clauirton@ci.ufpb.br, camila.barros@ci.ufpb.br)*

Abstract: This paper proposes a method that combines the Adaptive Perturb and Observe (Adaptive P&O) and Simulated Annealing (SA) optimization approaches to identify the global maximum power point in photovoltaic (PV) modules. This identification is critical to enable that such modules can deliver their maximum power to the utility network, considering different shading conditions. The Adaptive P&O method combines fast convergence and low steady-state oscillations, but it tends to return local rather than global maximum power values. Thus, it does not ensure the total efficiency of the modules. The SA approach is used to avoid this P&O limitation, creating a hybrid approach that explores the best features of each method. In order to test the proposed method, it has been applied to the Canadian Solar CSP-320 module under multiple shading by means of Matlab/Simulink simulations. Firstly, the module model was validated from its datasheet information, then, it was submitted to different shading conditions. Under these conditions, the proposed method converged to the maximum global power.

Keywords: Photovoltaic power, partial shading, adaptive P&O, optimization by simulated annealing.

1. INTRODUCTION

In 2017, the Brazilian power generation was formed by 65.5 % of hydropower plants, 6.9 % of PV and wind power plants, and 27.9% of other generation forms (e.g. thermal and nuclear) EPE (2019). In this same year, Brazil occupied the tenth position in the world ranking of countries that invested in PV energy generation. Thus, there is a high relevance in studies in this area, which can in fact support the expansion of this technology, mainly in a scenario of distributed microgeneration, which is one of the Smart Grid initiative principles.

The instability caused by shadings is one of the main problems of the PV generation. In cases of shading, the cells partially shaded act as a charge to the system, absorbing power and this process can warm and destroy the internal material of the cells (phenomenon is called *hotspot*). Bypass diodes are used to minimize these problems since they are able to isolate cells that are shading. Therefore, as the maximum power point (MPP) of PV modules is constantly changing in accordance with the shading condition, the MPP must also be continually recalculated.

The literature brings some works that propose strategies for maximum power point tracking of PV modules. The classical approaches are mainly based on variations of P&O that aim to mitigate its drawbacks (e.g. P&O oscillates around maximum point). The work of Abdelsalam et al. (2011), for example, proposes a technique that utilizes the rate of the array power change and treats it by a proportional-integral controller to generate an adaptive rather than a constant perturbation value. Similarly, the work of Ahmed and Salam (2015) employs a dynamic perturbation step-size to reduce the oscillation, while boundary conditions are introduced to prevent it from diverging away from the MPP. The work of Alik and Jusoh (2018) is another example. In this case, they use a checking algorithm to compare all peaks on the photovoltaic curve to clarify the global MPP. Apart from the P&O based techniques, other classical strategies to this problem are based on the Hill Climbing (Liu et al., 2008) and fractional open circuit voltage methods (Kobayashi et al., 2004).

The main limitation of these methods and their variants is that they are not able to reach global maximum power point in partial shading conditions since in such conditions there exist multiple local optimal in the power-voltage curve and these strategies generally converge into local rather than global optimal. Thus, recent investigations have been focused on different strategies, such as neural networks (Vasarevicius et al., 2012), (Rizzo and Scelba, 2015), which include parameters of the photovoltaic array (e.g. open circuit voltage), environment (e.g. radiation and temperature) and shading patterns as the typical attributes of their input layer.

Apart from the advantages of these more recent methods, P&O-based strategies are still the most used approach

to this domain, mainly due to its simplicity and low computational cost, which are very attractive features for systems that require fast response. The present study proposes a method that is also based on the P&O method. However, SA is integrated into the P&O with voltage adaptive step processing to avoid problems such as traps in local optimal. This problem is treated by the SA, that is known in literature to escape from local maximum value, to which the P&O is limited (Belhachat and Larbes, 2018). Therefore, the present study proposes a modification on the combined method P&O + SA, with the introduction of adaptive voltage step to P&O (Adaptive P&O).

The remaining paper is structured as follows: Section 2 presents the main concepts on the photovoltaic system model that was specified in this work. Section 3 summarizes the methods for maximum power point tracking, and related heuristics, which were adapted to compose the final proposal. Section 4 details the simulation and related tests, which use different shading configurations. Section 5 discusses the results of the tests and compares such results with other solutions of the literature. Finally, Section 6 brings conclusions and directions of research.

2. PHOTOVOLTAIC SYSTEM MODELLING

The modelling was based on the theoretical concepts of each system element, as detailed in the next subsections.

2.1 Photovoltaic Cell

The PV module consists of serial PV cells connections. The equivalent circuit that represents a PV cell is illustrated in Fig.1, based on the diode model (Ghani and Duke, 2011).

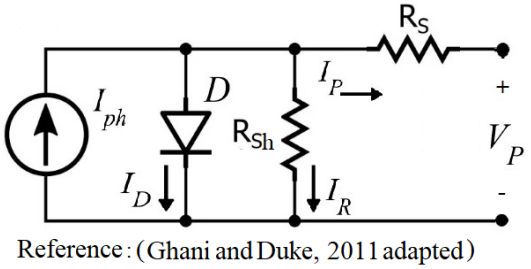

Figure 1. Electrical model of the photovoltaic cell.

In this schema, the current source I_{ph} represents the electrical current that is generated by the photovoltaic cell. This current is constant to a pre-defined irradiance and temperature. As the silicon is the material of this generator, it can be represented by a diode. I_D represents an unidirectional current that passes through this diode; V_p is the voltage in terminals of circuit; R_s and R_{sh} represent series and parallel parasite resistances, respectively.

The current I_p is determined as (1).

$$I_p = I_{ph} - I_D - I_R, \tag{1}$$

in which, the current I_{ph} are defined as (2).

$$I_{ph} = \frac{G}{G_R}(I_{sc}(1 + K_i(T_C - T_{C_R}))), \tag{2}$$

where G is the irradiance (W/m^2), G_r is the irradiance of reference (G_r = 1000 W/m^2), I_{sc} is the shortcut current; K_i is the coefficient of the shortcut current (K_i = 0,053 %/°C), T_C is the cell temperature in Kelvin (K), T_{C_R} is the cell reference temperature in Kelvin (K) (T_{C_R} = 298 K).

The current I_D is defined by (3).

$$I_D = I_o(e^{\left(\frac{V_{sh}}{mV_T}\right)} - 1), \tag{3}$$

in which, I_o is the diode saturation current, V_{sh} is the voltage in the parallel resistance, m is the idealist factor of the diode (m = 1,5), V_T is the thermal potential, represented by (4).

$$V_T = \frac{K.T_C}{q}, \tag{4}$$

where K is the Boltzmann constant ($K = 1,38.10^{-23}$ J/K), q is the electron charge ($q = 1,6.10^{-19}$ C).

I_R, the electrical current on parallel resistance, is given by (5).

$$I_R = \frac{V_p + R_s I_P}{R_{sh}}. \tag{5}$$

In addition, I_o is represented by (6).

$$I_o = I_{or}\left(\frac{T_C}{T_{C_R}}\right)^3 e^{\left(\frac{\epsilon_g}{m}\left(\frac{1}{V_{T_R}} - \frac{1}{V_T}\right)\right)}, \tag{6}$$

in which, I_{or} is the electrical reverse saturation current of the diode, ϵ_g is the energy gap of the silicon (ϵ_g = 1.11) and V_{T_R} is the thermal reference potential.

Finally, I_{or} and V_{T_R} are calculated by means of (7) and (8), where V_{oc} is the open circuit voltage.

$$I_{or} = \frac{I_{sc}}{e^{\left(\frac{V_{oc}}{mV_{T_R}}\right)} - 1}. \tag{7}$$

$$V_{T_R} = \frac{K.T_{C_R}}{q}. \tag{8}$$

2.2 Photovoltaic Module

The photovoltaic module was obtained from serial interconnection of a photovoltaic cells set. Such a simulated module refers to that of the Canadian Solar, of 320W (CS6U-320), composed of 72 cells, also connected in series (CanadianSolar, 2016).

In addition, studies under various shading conditions were performed in order to find the clustering of cells by bypass diodes that provided the maximum power supply. Thus, the clustering of 12 cells by bypass diode was founded. The Figure 2 show the simulated module PV.

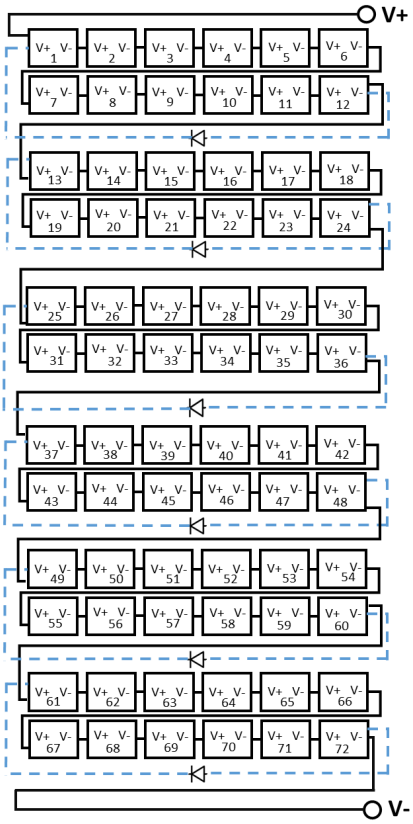

Figure 2. Photovoltaic Module.

3. PROPOSED METHOD FOR MAXIMUM POWER POINT TRACKING

The proposed method in this work consists in a combination of *Adaptive Perturb & Observe* (Ad. P&O) and *Simulated Annealing* (SA), which were integrated and applied to the task of MPP tracking.

The SA is based on the idea of the annealing in metallurgy, which involves heating and controlled a material cooling to increase the size of its crystals and reduce their defects, (Belhachat and Larbes, 2018). This method requires both the initial and final temperatures and a cooling rate as the input parameters. Applied to the PV modules context, this method consists of: random disturbances in the voltage supplied by the PV module and measurement of the associated electric current. With these values, it is calculated the supplied power and, if it exceeds the previous power value, the method takes its operating point to the voltage value that implies such higher power. Otherwise, it is calculated an acceptance probability (P_r) and, if it is higher than an value, randomly chosen in the interval [0, 1], the new operating point becomes this voltage value, even implying a reduction on the supplied power. This occurs to ensure that the method is able to escape the local maximums. This behaviour is mathematically represented in (9), where P_k is the power in the current voltage, P_i is the power associate to the voltage in the previous best operation point and T_k is the current temperature of the system. In addition, the cooling process is described in (10), where T_k reefers to the temperature related to the step k, T_{k-1}, to the value of temperature in the step $k-1$, and α is the cooling rate.

$$P_r = e^{\left(\frac{P_k - P_i}{T_k}\right)} \tag{9}$$

$$T_k = \alpha T_{k-1} \tag{10}$$

In addition, the Perturb and Observe (P&O) method is one of the most used technique for the maximum power point tracking problem. It is widely installed in commercial PV inverter using low cost microprocessors, (Ahmed and Salam, 2015). The main idea of this method is to perturb the voltage of the photovoltaic panel in a defined direction and to analyze the resultant power. If this power increases, then the voltage is still perturbed in the same direction. Otherwise, this direction is inversely modified. This process is repeated until a stop condition is reached.

Apart from its simplicity, P&O does not usually converge to the maximum power point since the generated perturbations cause an oscillation of the system around that point. Moreover, this method is not able to discern between global and local maximum points, so that its search is concluded when the first peak is found.

The P&O is used as complementary method to SA. However, an improvement is made on this method, with the inclusion of adaptive voltage step. The adaptation cited refers to the fact that great values of voltage step, when more far from the Maximum Power Point (MPP), implies higher convergence speed. This perturbation to voltage step is reduced, when the MPP is closer, allowing the reduction of oscillations around him. The P&O with this improvement is known as Adaptive Perturb and Observe (Ad. P&O).

It is important to highlight that this voltage adaptive relation is expressed in (11). This equation shows that the adaptive voltage step (Δv), referent to Ad. P&O method, is proportional to (12):

$$\Delta v = M \frac{\Delta P_k}{\Delta V_k} \tag{11}$$

$$\frac{\Delta P_k}{\Delta V_k} = \frac{|P_{p(k)} - P_{mpp}|}{|V_{p(k)} - V_{mpp}|} \tag{12}$$

Being $P_{p(k)}$ and $V_{p(k)}$ the current power and voltage values, respectively; P_{mpp} and V_{mpp} the power and voltage values in the MPP, considering G = 1000 W/m^2 and T = 25°C and M the proportionality constant. Finally, after Δv calculation, it is applied to the current voltage value, representing the voltage perturbation inherent to the method in question in this section, as indicate in (13).

$$V_{p(k+1)} = V_{p(k)} + \Delta v * slope \tag{13}$$

In which $V_{p(k)}$ is the current voltage value, $V_{p(k+1)}$ is the voltage value in next simulation step, Δv represents the adaptive voltage step and *slope* indicates the signal, positive or negative, that is applied to Δv.

In brief, while the Simulated Annealing accounts for finding the voltage value in the region of global maximum power, the Adaptive Perturb & Observe conducts the refinement of this value so that it can be as much as possible

closer to the optimal global power. The Fig. 3 shows the schematic of the PV module with MPPT based on SA + Ad. P&O, in which it is perceived that the SA provides the Ad. P&O with a voltage value in the vicinity of the optimum voltage, that implies the maximum power and to be found by the second method (Ad. P&O). Moreover, the Fig.4 shows the flowchart of proposed method (SA + Ad. P&O)

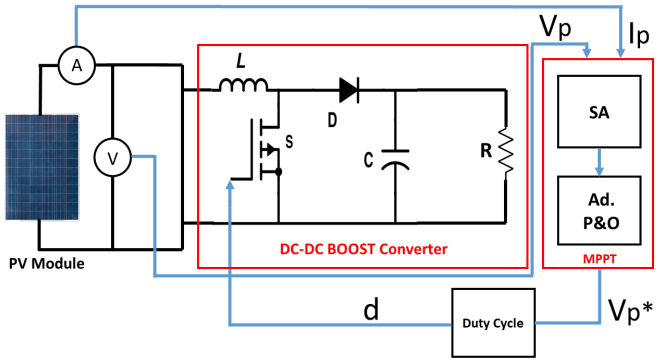

Figure 3. Schematic of the PV module with MPPT based on SA + adaptive P&O.

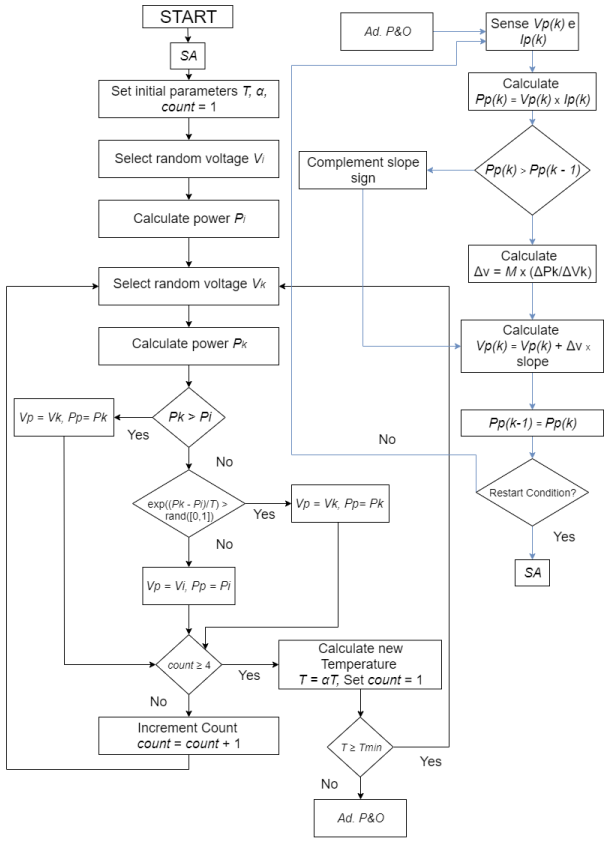

Figure 4. Flowchart of SA + adaptive P&O method.

The joint use of the Ad. P&O and SA methods affects the search so it is not limited to a local optimal solution, providing a global vision of the problem to the controller, which takes advantage of the fast execution and low complexity of both methods. Importantly, the global search (SA) method is triggered whenever there is a power variance above a threshold, whose value was equal to 10%. This drive technique is indicated in (14).

$$\frac{|P_{current} - P_{previous}|}{P_{previous}} * 100 \geq threshold \qquad (14)$$

4. TEST SYSTEM

The simulations described in this section have been developed in MatLab/Simulink, based on system modeling. The parameters were extracted of Canadian Solar CS6U-320 (320 W) model datasheet, (CanadianSolar, 2016), and will be described in section 4.1. In addition, the section 4.2 explicit the values of boost converter components, the section 4.3 described the procedure for determining the number of bypass diodes and, finally, in the section 4.4, the shading conditions simulated in this study are discussed.

4.1 Model Parameters

As the model of the PV module was the *Canadian Solar* (CS6U-320, 320 W), the test parameters was extracted from its datasheet (CanadianSolar, 2016), in which the short circuit current (I_{sc}), open circuit voltage (V_{oc}) and temperature coefficient are equal to 9.26 A, 45.3 V and 0.053%/°C, respectively.

In addition, the values of the parasite resistances in series (R_s) and *shunt* (R_{sh}) were, respectively, 0.0046 Ω and 4.8611 Ω, obtained experimentally. As the cells of the panel are connected in series, then the open circuit voltage to one cell can be obtained by means of the quotient between the open circuit voltage of the panel (V_{oc} = 45.3 V) and the number of cells (n = 72); while the shortcut current of each cell is the same than the current of the panel (I_{sc} = 9.26 A).

Finally, the P_{mpp} and V_{mpp} values, also extracted from the datasheet (CanadianSolar, 2016), was 300 W and 36.8 V (36 V), respectively, and the constant M, obtained experimentally, was equal to 0.0005.

4.2 Boost Converter

The present section discusses the DC-DC Boost Converter (Fig.3) project. Thus, considering the maximum power (P_{mpp}) equal to 300 W and determining that the load voltage (V_{Load}) is equal to 100 V, the load resistance value is described in (15).

$$R = \frac{V_{Load}^2}{P_{mpp}} = \frac{100^2}{300} = 33.33\Omega \qquad (15)$$

In order to calculate the inductor value, it is considered the V_{mpp} value obtained from datasheet, CanadianSolar (2016), equal to 36.8 V (36 V, approximately). From this value, the duty cycle (d) is equal to 0.64. Thus, considering a boost work frequency (f_s) equal to 5 KHz, that imply a period (T_s) equal to 200 μs, and an oscillation on inductor current Δi_L equal to 100 mA, project parameter, the inductance value is described on (16).

$$L = \frac{V_{mpp} dT_s}{\Delta i_L} = \frac{36 * 0.64 * 200 * 10^{-}6}{100 * 10^{-}3} = 46.08mH \quad (16)$$

Its is important to highlight that the inductor value was approximated to 50 mH. Finally, knowing that the load current (I_{Load}) is expressed by (17) and that the oscillation on capacitor voltage ΔV_C is equal to 1 V, project parameter,

$$I_{Load} = \frac{V_{Load}}{R} = \frac{100}{33.33} = 3A \quad (17)$$

The capacitance value is equal to (18)

$$C = \frac{I_{Load} dT_s}{\Delta V_C} = \frac{3 * 0.64 * 200 * 10^{-}6}{1} = 384\mu F \quad (18)$$

With the capacitor, inductor and load values determined, the DC-DC BOOST project is finished.

4.3 Addition of the Bypass Diode

A *Bypass* diode was placed into each group of twelve cells so that it could conduct the electrical current in shading situations. This number of cells was empirically defined after experiments with groups of 1, 2, 3, 4, 6, 8, 9, 12, 18, 24 e 36 cells per diode. Three experiments were conducted for each of these groups. The first experiment shaded 12 cells, the second experiment shaded 36 cells and, finally, the last experiment shaded 60 cells. Two values of irradiance were used: 500 W/m^2 e 750 W/m^2. Thus, we executed 66 different experiments (11 groups x 3 shading configurations x 2 values of irradiance). After these tests, we concluded that the group of 12 cells per diode was the best option in terms of performance, because the highest power values were obtained in this scenario.

4.4 MPP Tracking in Partial Shading Conditions

The values used in the experiments were 900°C to the initial temperature, 0.02°C to the final temperature and 0.9 to the cooling rate (α), used in SA. In addition, three shading conditions were tested, conditions 1 (C1), 2 (C2) and 3 (C3), which are shown in Fig.5(a), Fig.5(b) and Fig.5(c), respectively. Each matrix represents the 72 cells PV module, and such cells are organized in a 12x6 arrangement. Its elements (a_{ij}) have an irradiance value (W/m^2) that corresponds to the cell in the position ij. All conditions were dynamically tested with simulation time for each of them equal to 0.6 s, respectively, and transitions times equal to 0.0001 s between them.

The curves PxV (Power x Electrical voltage) related to the conditions C1, C2 and C3 are also presented in Fig.5(a), Fig.5(b), Fig.5(c), whose maximum local (P1) and global (P2) power values are equal to, respectively, 131.6 W, 163.1 W for C1; 131.7 W, 239.5 W for C2 and 242.9 W, 255.4 W for C3.

5. RESULTS AND DISCUSSIONS

The PV cells were specified using the equations of the photovoltaic cell model (Section 2.1), which form the PV

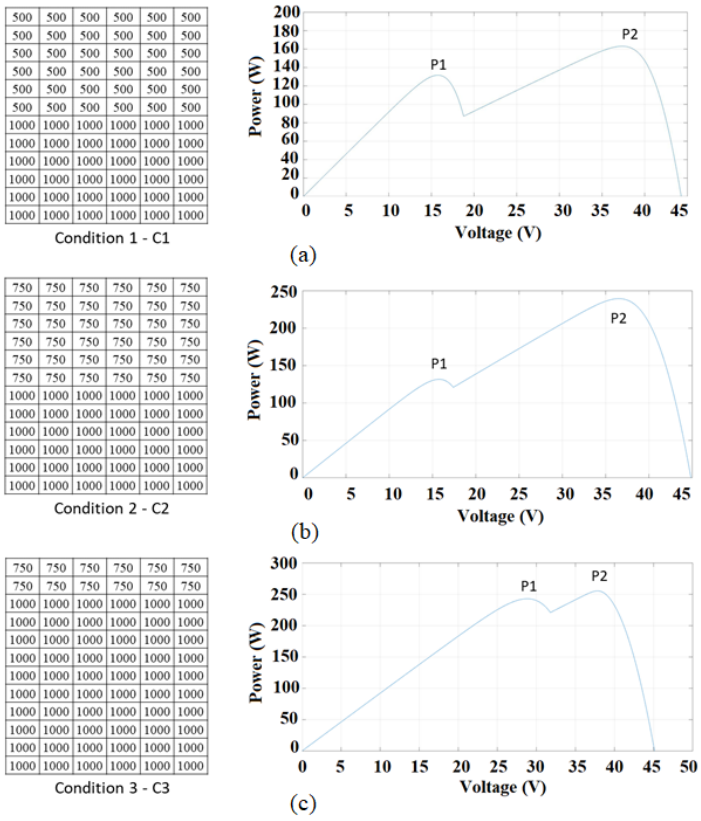

Figure 5. Simulated shading conditions and correspondents Power x Voltage curves, C1 (a), C2 (b) and C3 (c), respectively.

module. To that end, the *Canadian* solar module CS6U-320 of 320 W was used as test system. This module has 72 cells placed into a matrix of 12x6 (CanadianSolar, 2016). These cells are interconnected by means of a serial connection.

Considering the shading conditions C1, C2 and C3, the Fig.6(a) presents the curves V_p x Time, the Fig.6(b) presents the curves I_p x Time and the Fig.6(c) presents the curves P_p x Time for proposed method and Ad. P&O. Specifically, Fig.6(c) shows that the proposed method obtained a better performance when compared to the P&O approach, because it found the maximum power value on all shading conditions tested, while the Ad.P&O did not exceed the local maximum values. This analysis is complemented by Fig.6(a) and Fig.6(b), which show the current (I_p) and voltage (V_p) values as a function of time.

The tests show that the proposed method was more efficient to search the global maximum power point when compared to the Ad. P&O. Its limitation is related to the local maximum problem. This means, there is not a global vision of the problem and, consequently, the algorithm just finds a local maximum regarding a specific neighborhood. The proposed method (Ad. P&O + SA) is used to overpass this limitation. SA provides, as a start point to Ad. P&O, a voltage value that is part of the neighborhood where the global maximum value is. Thus, Ad. P&O is able to find this value.

Finally, Fig.6(c) shows the actuation of global search restart condition (14). At times 0.6 s and 1.2 s, occur

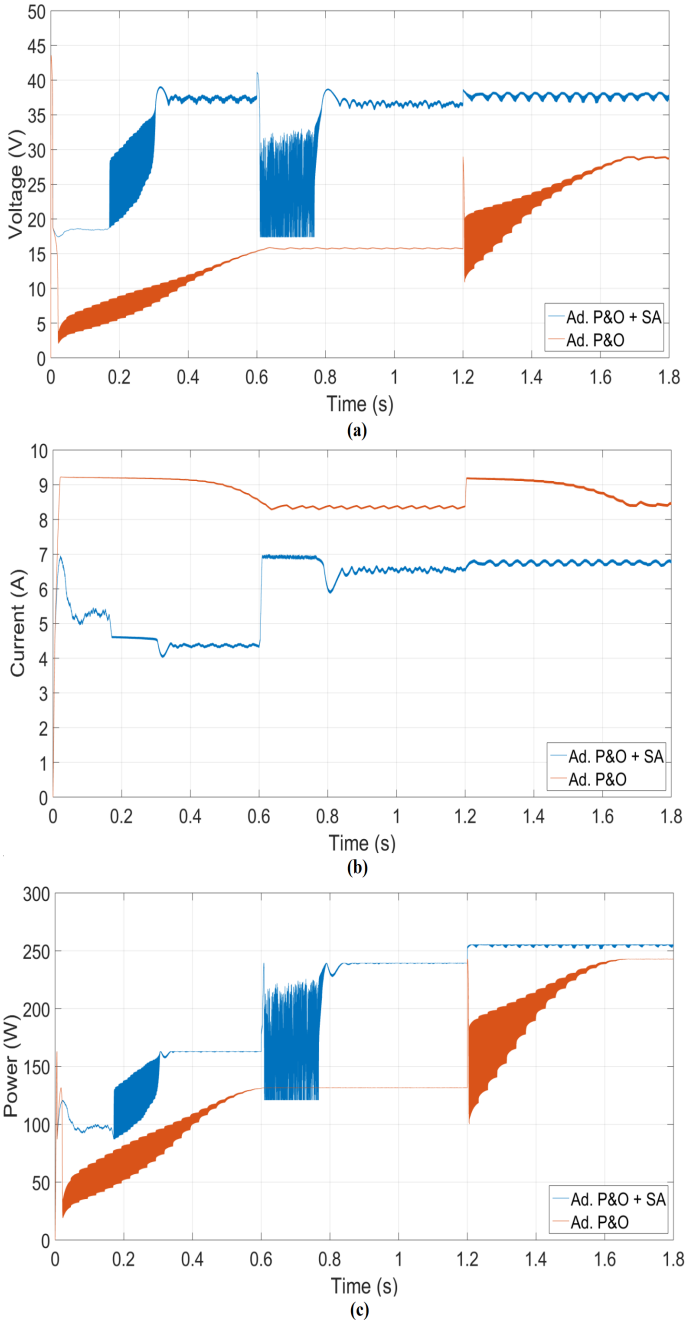

Figure 6. Voltage x Time (a), Current x Time (b) and Power x Time (c) resultant curves from the shading conditions execution.

two shading conditions changes (C1-C2 and C2-C3), respectively. The first was detected by condition, because it implied a power variation higher than 10%, while the second is not detected. This no detection is justified by the fact that power variation, originated of shading condition change (C2-C3), is low enough to avoid the global search restart. In this case, it is likely that the Ad. P&O is able to find the maximum power value. Thus, a more sophisticated search is not necessary, as proposed by the SA.

6. CONCLUSIONS AND RESEARCH DIRECTIONS

The proposed method obtained better results when compared to the individual executions of the P&O approaches. However, comparisons with other search techniques are required, in order to corroborate the good results obtained with this hybrid method. Moreover, it is intended to perform the simulated tests on a real PV module, because practical results are important for the enrichment of the work developed.

Finally, an improvement to be included consists in the decrease of the oscillations in the voltage and, consequently, in the power provided by the PV module. Abrupt changes in the reference voltage, supplied by the MPPT, cause the output voltage of the BOOST converter to oscillate more significantly. Therefore, alternatives that minimize the negative effects of these situations can be sought, which is a starting point for future researches.

REFERENCES

Abdelsalam, A.K., Massoud, A.M., Ahmed, S., and Enjeti, P.N. (2011). High-performance adaptive perturb and observe MPPT technique for photovoltaic-based microgrids. *IEEE Transactions on Power Eletronics*, 26(4), 1010–1021.

Ahmed, J. and Salam, Z. (2015). An improved perturb and observe (P&O) maximum power point tracking (MPPT) algorithm for higher efficiency. *Applied Energy*, 150, 97–108.

Alik, R. and Jusoh, A. (2018). An enhanced P&O checking algorithm MPPT forhigh tracking efficiency of partially shaded pv module. *Solar Energy*, 163, 570–580.

Belhachat, F. and Larbes, C. (2018). A review of global maximum powerpoint tracking techniques of photovoltaic system under partial shadingconditions. *Renewable and Sustainable Energy Reviews*, 92, 513–553.

CanadianSolar (2016). MAXPOWER CS6U-315|320|325|330P. <http://download.aldo.com.br/pdfprodutos/Produto34009IdArquivo4019.pdf>. [Online] Acessado em: 13/04/2019.

EPE (2019). Energy and electrical matrix. <http://www.epe.gov.br/pt/abcdenergia/matriz-energetica-e-eletrica>. [Online] Acessado em: 02/03/2019.

Ghani, F. and Duke, M. (2011). Numerical determination of parasitic resistances of a solar cell using the lambert w-function. *Solar Energy*, 85, 2386–2394.

Kobayashi, K., Matsuo, H., and Sekine, Y. (2004). A novel optimum operating pointtracker of the solar cell power supply system. *Proceedings of the 2004* IEEE *35th annual power electronics specialists conference. PESC 04*, 2147–2151.

Liu, F., Kang, Y., Zhang, Y., and Duan, S. (2008). Comparison of P&O and hillclimbing MPPT methods for grid-connected PV converter. *Proceedingsof the 3rd IEEE conference on industrial electronics and applications. ICIEA 2008, IEEE*, 804–807.

Rizzo, S.A. and Scelba, G. (2015). Ann based mppt method for rapidly variableshading conditions. *Appl Energy*, 145, 124–132.

Vasarevicius, D., Martavicius, R., and Pikutis, M. (2012). Application of artificial neural networks for maximum power point tracking of photovoltaic panels. *Electronics and Electrical Engineering*, 18.